

A Switched-Winding Transformer with Low Quiescent Loss to Meet the Level VI Efficiency Standard at High Power Density

Weston Braun¹, Minjie Chen², and David J. Perreault¹

¹Massachusetts Institute of Technology, Cambridge, MA, 02139, USA

²Princeton University, Princeton, NJ, 08540, USA

Abstract—Many control and monitoring applications including thermostats, doorbells, and security systems utilize 60 Hz transformers with grid-voltage inputs and 16 V to 24 V ac outputs. The new DOE Level VI efficiency standard places stringent requirements on the no-load quiescent loss of grid-interface power supplies, including these low-voltage transformers. This paper explores a low-cost but highly effective approach to reduce the quiescent loss and improve the power density of these transformers while meeting the Level VI efficiency standard. By reconfiguring windings based on the operating power level, one can achieve higher average efficiency, lower quiescent loss, and higher power density. It is experimentally demonstrated that compared to a conventional transformer design that meets the new Level VI standard, the proposed switched-winding transformer approach can more than double the achievable transformer power rating at the same size, weight and core, while requiring only a modest increase in complexity.

I. INTRODUCTION

GRID-interfaced ac-dc power supplies have been widely implemented as switch-mode power converters. However, off-grid power supplies for many miscellaneous control systems - e.g. thermostats, doorbells, security systems - still utilize line-frequency transformers as ac-ac power supplies. The new DOE Level VI efficiency standard [1] (Table I) places stringent requirement on the light load/quiescent loss of grid-interface power supplies, including such transformers. This standard regulates both the no-load loss and the average efficiency (four-point arithmetic average of efficiencies at 25%, 50%, 75% and 100% load) as a function of power rating. Table II compares the measured performance of a few 120 Vac commercial transformers against the new Level VI efficiency standard. As shown in the table, some of the tested transformers are able to meet the Level VI efficiency requirement, but none meet the no-load loss requirement which is predominately a function of core loss.

The total loss in a transformer can be divided into core loss and copper loss. In an optimized design copper loss and core loss have to be jointly considered. Core loss is the primary component of the no-load loss, while copper loss is the primary loss under load and thus has the biggest impact on loaded efficiency and power rating. Minimizing one of these losses requires tradeoffs in terms of the other or the overall volume of the transformer. For a given transformer weight or size, one can adjust the number of turns and the core size to benefit core loss or winding loss (and loaded efficiency) at the expense of the other. Imposing both tight no-load loss

TABLE I
LEVEL VI EFFICIENCY STANDARD ON SINGLE VOLTAGE EXTERNAL AC-AC POWER SUPPLY

Nameplate Power	Output	Minimum Average Efficiency	Maximum Power in No-Load Mode
$P_{out} \leq 1W$		$\geq 0.517 \times P_{out} + 0.087$	≤ 0.210
$1W < P_{out} \leq 49W$		$\geq 0.0834 \times \ln(P_{out}) - 0.0014P_{out} + 0.609$	≤ 0.210
$49W < P_{out} \leq 250W$		≤ 0.870	≤ 0.210
$P_{out} > 250W$		≤ 0.870	≤ 0.210

TABLE II
MEASURED PERFORMANCE OF COMMERCIALY AVAILABLE TRANSFORMERS

Brands	Triad 3W	CUI 6W	CUI 12W	Triad 18.8W	Triad 43.2W
Measured No Load Loss	0.461W	0.354W	0.383W	1.992W	0.863W
Required No Load Loss	0.210W	0.210W	0.210W	0.210W	0.210W
Measured Average Efficiency	73.8%	79.3%	82.7%	77.5%	90.4%
Required Average Efficiency	69.6%	75.0%	79.9%	82.7%	86.2%

limits and loaded efficiency requirements greatly restricts the achievable power level for a given transformer size.

The Level VI efficiency standard poses a particular challenge as both the loaded efficiency and no-load loss of transformers needs to be improved. The traditional approach of having core size being saturation limited for small line-frequency transformers has been largely acceptable for the previous mandates on no-load power consumption. However, under the Level VI standard, core loss under no-load conditions represents a significant new design constraint. When imposed along with the increase in loaded efficiency requirements this greatly limits the achievable power density. However, this new efficiency standard opens new design opportunities to apply switched transformer and inductor techniques that have previously been utilized in dc-dc converter applications [2], [3], VCOs in integrated circuits [4], [5], energy harvesting [6], and PFC converters [7], to enhance traditionally fully-passive line-frequency transformers.

This paper explores a cost-effective approach to improving the performance of line-frequency transformers, resulting in larger power capability for a given transformer size while meeting no-load loss and average efficiency requirements. The proposed approach, similar to a previously developed approach as presented in literature [8], utilizes a reconfigurable transformer with identical pairs of primary and secondary windings. The electrical connections within each of these winding pairs are reconfigured depending on the load condition. Under light load, the two winding pairs are each connected in series to reduce the core loss at the cost of increased copper loss; under heavy load, the two winding pairs are each connected in parallel to reduce the copper loss at the cost of an increased core loss. This additional configuration allows for the partial decoupling of core loss at light load and copper loss under heavy load, enabling significant improvements in transformer efficiency and power density to fulfill both the no-load and loaded efficiency requirements. While this concept has been proved effective in medium power motor drive applications (around 500VA in [8]), we present a simple but very effective approach to implement the sensing and control circuit for low power applications under 50VA (i.e., power supplies for security cameras), and experimentally demonstrate the effectiveness of the approach by adopting 3D-printing technology and miniaturized system packaging.

II. SWITCHED-WINDING TRANSFORMER SYSTEM

Figure 1 illustrates the basic concept of the proposed switched-winding transformer system. A switched-winding transformer comprises two primary windings, two secondary windings, and a switching network with associated control circuitry that can simultaneously reconfigure the two pairs of windings in series or parallel depending on the load condition. In heavy load, the relays are configured in T1 positions to connect windings in parallel and reduce the winding loss. In light load, the relays are configured in T2 positions to connect windings in series to reduce the core loss.

Figure 2 provides a cross sectional view of a switched-winding transformer. A switched-winding transformer can be interpreted as a modified single-winding ac-ac transformer with the same core geometry but split primary and secondary windings. Under light load, the two windings pairs are connected in series and the system behaves the same as a traditional transformer that had been optimized with low core loss to meet the no-load loss requirements. Under heavy load, the two windings are connected in parallel and the system behaves as a transformer optimized to reduce heavy-load winding loss. As the reduction in copper loss is much larger than the increase in core loss this allows for an increased power rating or power density.

III. SCALING FACTOR ANALYSIS

The performance of a magnetic element is analyzed following the theoretical methods presented in [9], [10]. This analysis is presented as a set of scaling equations which relate the core loss and winding resistance, or copper loss, of a transformer to its volume and number of turns. For the

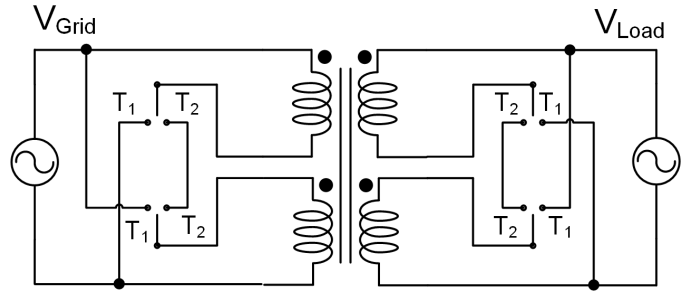


Fig. 1. Basic concept of the switched-winding transformer architecture.

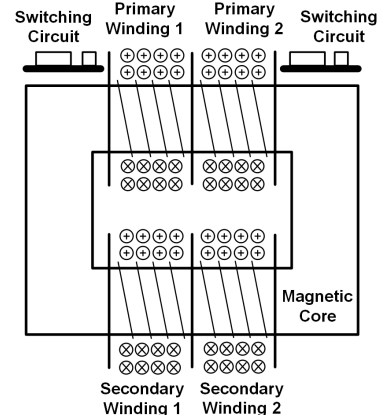


Fig. 2. Cross section view of the proposed switched-winding transformer.

purpose of the analysis, it is assumed that core loss is the only loss in no-load conditions and copper loss is the only loss under loaded conditions. The assumption about no-load conditions leads to little error as the primary current under no-load conditions consists only of the magnetizing current and there is no secondary current. The assumption that copper loss is the only loss under loaded conditions can lead to some error for transformers with very high core loss. The derived set of equations will allow for direct comparison of the switched-winding approach with traditional transformers that do not use the switched-winding approach.

A fixed aspect ratio transformer has two degrees of freedom in its design: a linear scaling factor applied to each dimension, which we can call α , and a scaling factor for the number of turns, n . Starting from the fixed and known winding resistance and core loss of a given transformer we can model the winding resistance and core loss of a new scaled transformer with a different linear scaling factor and number of turns.

Based on the Steinmetz equation, for a fixed line frequency (i.e, 60Hz in the US), core loss can be estimated as a function of B_{max} , α , and n :

$$\begin{cases} P_{core} \propto B_{max}^m \times \alpha^3 \\ B_{max} \propto n^{-1} \times \alpha^{-2} \\ P_{core} \propto n^{-m} \times \alpha^{3-2m} \end{cases} \quad (1)$$

Where m is the Steinmetz constant, which is in the range between 1.8 and 2.2 for most silicon steels [11]. B_{max} is inversely proportional to both the number of turns and core

cross section area. The winding resistance, which is directly proportional to the copper loss, can be modeled as n turns of length proportional to α and cross sectional area proportional to the area of the winding window divided by n :

$$P_{copper} \propto n^2 \times \alpha^{-1} \quad (2)$$

Intuitively, the length of the winding is proportional to n , the resistance per length of the winding is proportional to n (decreasing cross-sectional area as n increases), the resistance per length of the winding is inversely proportional to α^2 (increasing cross section area as α increases), and the length per turn of the winding is proportional to α .

Treating n as a dependent variable between (1) and (2), two equations can be derived which relate the scaling factor α to either core loss or copper loss while the other remains constant.

If copper loss remains constant, the core loss is:

$$P_{core} \propto \alpha^{3-5/2m} \quad (3)$$

If core loss remains constant, the copper loss is:

$$P_{copper} \propto \alpha^{-5+6/m} \quad (4)$$

A more useful form of this derivation is when the change in core volume is expressed as a function of the scaling factor, relating the desired copper loss or core loss to the existing copper loss and core loss. This can be achieved by replacing the dimensional scaling factor α with a volume scaling factor ($\alpha^3 \propto V$) and rearranging the equations:

$$V \propto P_{core}^{6/(6-5m)} \quad (5)$$

$$V \propto P_{copper}^{3m/(6-5m)} \quad (6)$$

In practical designs, given the range of m for common silicon steels (i.e., $1.8 < m < 2.2$), the empirical estimation of the volume of a transformer as a function of the core loss or copper loss would be:

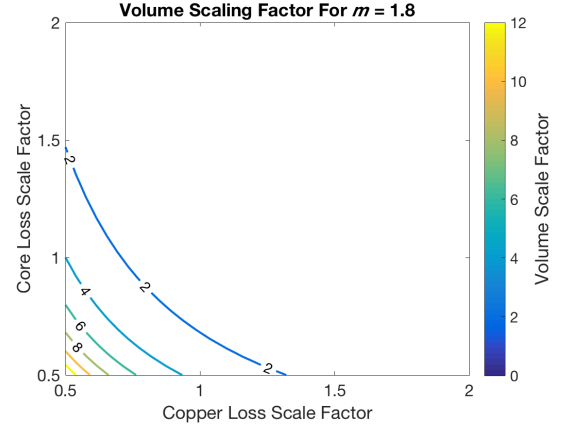
$$V \propto [P_{core}^{-2}, P_{core}^{-1.2}] \quad (7)$$

$$V \propto [P_{copper}^{-1.8}, P_{copper}^{-1.32}] \quad (8)$$

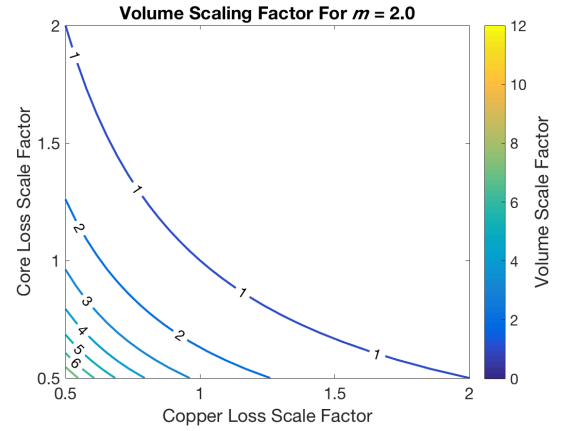
Based on this model many of the tested transformers would need to more than double in volume to meet the Level VI no load power consumption specification (as shown in Table II) to reduce the loss by half.

Figure 3 illustrates this relationship for $m = 1.8, 2.0,$ and 2.2 , respectively. These charts can be utilized as a reference for optimizing the core loss, copper loss, and size of a transformer. For example, for a magnetic material with $m = 2.0$ (Figure 3b), while keeping the copper loss constant, one would need to increase the core loss by a factor of 3 to halve the overall volume.

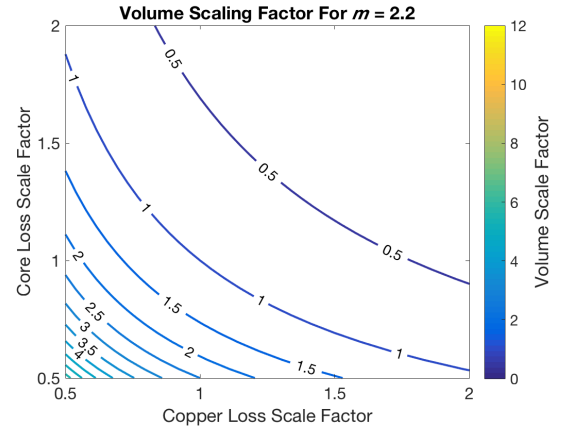
The proposed switched-winding system configures a pair of windings in series under low load conditions. This leads to a 2x reduction in the volts per turn applied to the core and



(a)



(b)



(c)

Fig. 3. Quantitative tradeoff analysis between copper loss and core loss for (a) $m=1.8$, (b) $m=2.0$, (c) $m=2.2$.

thus a 2x reduction in B_{max} . The reduction in no-load power consumption achievable with the switched-winding system can be translated into a volume savings when compared to a traditional transformer by using the previously derived equations. The difference in the magnetic field strength between the switched-winding transformer in its low-power state (with two windings in series) and the high-power state (with two windings in parallel) can be expressed as:

$$\frac{B_{max,high-power}}{B_{max,low-power}} = 2 \quad (9)$$

And the ratio between the core losses is:

$$\frac{P_{core,high-power}}{P_{core,low-power}} = 2^m \quad (10)$$

For m between 1.8 and 2.2, this ratio falls in the range between 3.48 to 4.59. As a traditional transformer cannot change its core loss the one operating point needs to meet both the Level VI no-load and efficiency requirements. The proposed switched-winding topology operates in two modes that cover two points in the tradeoff between core loss and copper loss. In one mode the system only needs to meet the Level VI no-load requirement and in the other mode the system only needs to meet the Level VI efficiency requirement. In comparison, the copper loss of the switched-winding transformer in the high power mode is equal to the copper loss of the traditional transformer. The core loss of the switched-winding transformer in low power mode is equal to the core loss of the traditional transformer. The switched-winding transformer can be compared to the traditional transformer by viewing it as a transformer with identical copper loss but core loss that is proportionally greater:

$$\frac{P_{core,switched-winding}}{P_{core,traditional}} = 2^m \quad (11)$$

The previously derived relationship between P_{core} and volume can then be used to establish a relationship between the volume of the switched winding transformer and the traditional transformer:

$$\frac{V_{switched-winding}}{V_{traditional}} = (2^m)^{6/(6-5m)} = 2^{6m/(6-5m)} \quad (12)$$

For the given range of m this equates to a ratio between 0.082 and 0.160. This represents a potential volume savings of at least 600%.

However, this model assumes that core loss is negligible compared to copper loss under heavy load, an assumption that may not hold true for large values of core loss. Additionally, small transformers may be flux density limited by saturation in the high power mode when designed for a low power mode core loss equal to the Level VI no-load limit, preventing the full scaling from being achieved. For low power applications the implementation of the control circuitry and the packaging of the multiple windings are also critical in minimizing the overall system volume. Nevertheless, this analysis gives us a good reference in making tradeoffs between copper loss and core loss when designing a miniaturized low voltage transformer.

IV. PROTOTYPE

A prototype switched-winding transformer meeting the Level VI requirements has been constructed along with a conventional comparison transformer using the same core set and bobbins of similar size. Figure 4 provides a simplified schematic of the full prototype including the control circuitry.

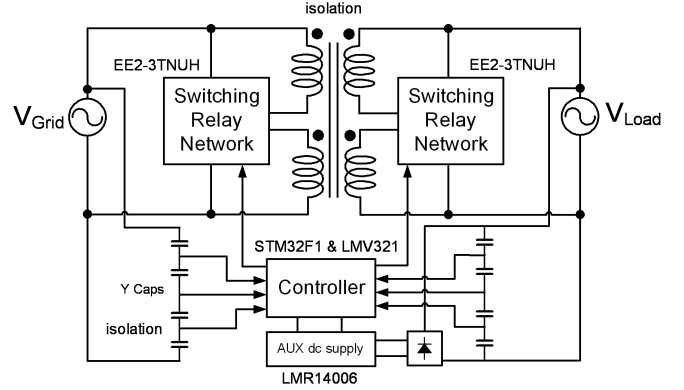


Fig. 4. Simplified schematic of the full prototype.

The switched-winding system and comparison transformer were designed for a 120V 60Hz line voltage and nominal output voltage of 24V. Exact output power was determined from the measured output characteristics and the Level VI efficiency requirements, but the designed target output power was 40-50W. The switched-winding system consists of a dual-primary dual-secondary transformer and a STM32F0 microcontroller based control circuit, which monitors the output power and reconfigures the transformer connections for optimal performance.

The control circuit monitors the output power of the switched-winding transformer by utilizing the winding resistance of the transformer as a current sense resistor. This method is similar to the method of measuring the average DC voltage across an inductor resulting from the IR voltage drop to measure average current. However, in a transformer there is no average DC current and thus the average IR voltage is zero. This means that the IR voltage drop must be measured at the line frequency as it is in phase with the transformer output voltage and superimposed on the output voltage waveform. Given a known value for the transformer open circuit output the IR voltage drop could be derived by subtracting out the open circuit voltage from the measured secondary voltage. However, fluctuations in the line voltage make this method inaccurate and unreliable. Instead both the transformer primary and secondary voltage is measured and the ratio between them is used.

Two differential amplifiers utilizing a commodity opamp (LMV321) are used on the primary and secondary side of the transformer to measure the input and output voltages through capacitive dividers. Y rated capacitors are used on the primary side voltage divider to ensure isolation from the AC line. The two voltages are digitized with the microcontroller's internal ADC and several samples are taken over each AC cycle. The ratio between these samples is calculated and passed through a digital Infinite Impulse Response (IIR) filter for increased noise immunity. Given the resolution of the microcontroller's ADC, the input voltage limit, and a predicted maximum output voltage drop of 20% under load, this measurement method for output power has a resolution of approximately 7 bits. Due to the temperature coefficient of the copper windings, the accuracy of this measuring method may vary up to 30% under

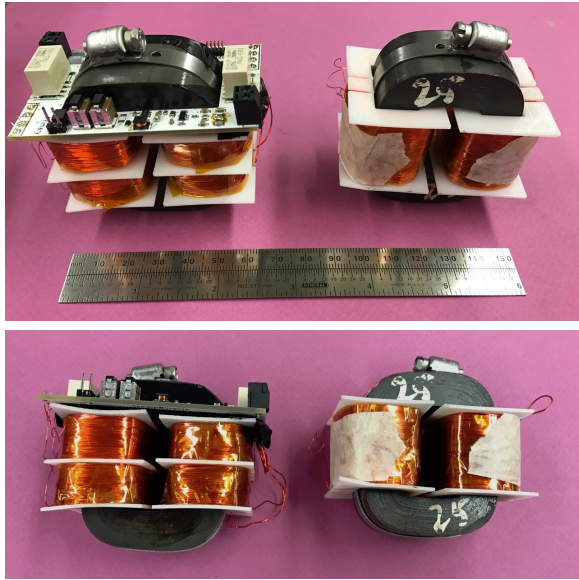


Fig. 5. Pictures of the prototypes: Left: switched winding transformer; Right: comparison transformer. 6" ruler for scale.

operating temperature range. However, the system is robust against this variation as the metric that needs to be acted upon is system efficiency, which is still accurately measured despite changes in winding resistance.

The transformer is reconfigured using latching relays (EE2-3TNUH) for their robustness, simple drive requirements, low loss, and surge current capability. A transition between power states of the transformer is triggered when the microcontroller calculates that the system would perform better in another state based on the measured output power. To reduce switching transients, the system switches at the peak of the AC voltage cycle. This approach minimizes the energy stored in the transformer magnetizing inductance when switching from the high power mode to the low power mode and reduces the volt \times second imbalance that could cause saturation of the core and possibly damaging currents when switching from low power mode to high power mode.

The phase angle of the switching is controlled by entering a high ADC sample rate mode and waiting for a zero crossing. Once a zero crossing is detected the microcontroller delays a fixed time before switching the relay such that the relay contacts will actuate at the desired part of the line cycle. By predicting the occurrence of the desired switching point instead of switching after observing it, the delay due to the relay switching time can be mitigated. Additionally, detecting a zero crossing is more robust to fluctuations in variations in line voltage and noise than directly detecting an arbitrary point of the AC cycle.

Hysteresis is required in the control loop for switching between high and low power states due to the difference in output impedance between the two states. Due to the parallel series configuration, the low power state has approximately 4x the winding resistance of the high power state. When loaded with a constant resistance load this leads to differences in output voltage and power between the two states. If the load

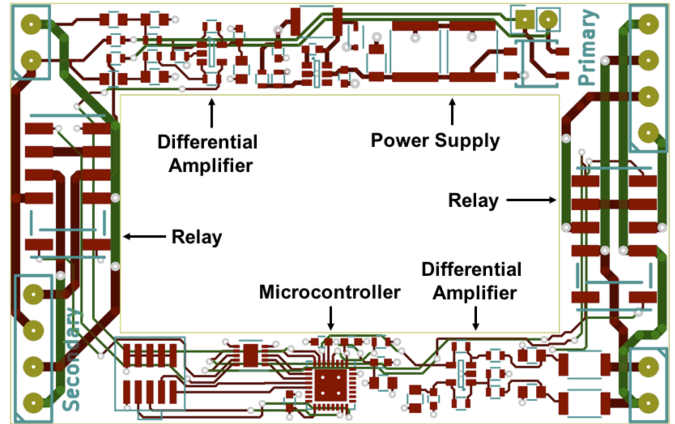


Fig. 6. Component layout of the control printed circuit board.

point is close to the transition point between states this can lead to oscillation between the two states.

Power for the control circuitry is provided from the secondary windings of the switched-winding transformer. The nominal voltage of 24 Vac is rectified and filtered with an array of ceramic capacitors. The voltage is then stepped down to 3.3V to support the microcontroller and analog circuitry via a low quiescent loss buck converter (LMR14006). This electrolytic-free auxiliary power supply ensures long life at high temperatures. Drawing power from the transformer itself reduces the cost and complexity of the design but also means that the power drawn by the controller becomes part of the limited no-load power consumption budget. In this prototype, the analog circuitry used to measure the output power of the transformer draws less than 1 mW. The majority of the power is drawn by the microcontroller. Through the use of sleep modes and a reduced system clock the total power drawn by the control circuitry is limited to less than 10mW. It is important to minimize the power drawn by the control circuitry as it directly impacts the allowed core loss and thus the overall size of the system. The 10mW drawn by the control circuitry represents less than 5% of the total no load power consumption and any further reduction represents a domain of diminishing returns.

Photographs of the prototyped switched-winding transformer and the comparison transformer are provided in Figure 5 while Figure 6 provides a rendering of the control PCB. The control board was designed as a rectangular cutout, allowing it to fit over the transformer core and sit atop the primary and secondary bobbins, significantly decreasing the bounding box. Custom transformer bobbins were designed in OpenSCAD and 3D printed in ABS plastic. The switched-winding transformer utilizes a two segment bobbin to accommodate the dual primary and secondary windings while the comparison transformer employs a single segment winding. Table III shows the specifications of the two transformers.

V. EXPERIMENTAL RESULTS

The average efficiency and no-load loss of both the switched-winding transformer and the comparison transformer

TABLE III
PROTOTYPE TRANSFORMER SPECIFICATIONS

Specification	Comparison Transformer	Switched-Winding Transformer
Core	CD12.5x25x30	CD12.5x25x30
Primary Turns	1700 Turns	900 Turns x2
	30AWG	30AWG
Secondary Turns	340 Turns	180 Turns x2
	24AWG	24AWG
Volume (in ³)	11.95	14.15
Mass (g)	485.4	512.6

TABLE IV
PERFORMANCE OF SWITCHED-WINDING TRANSFORMER AND COMPARISON TRANSFORMER

Tested Transformer	Prototype	Conventional
Average Efficiency (%)	87.7%	86.7%
No-Load Loss (W)	0.192	0.168
Rated Power (W)	43	16
Power Density (W/in ³)	3.04	1.34

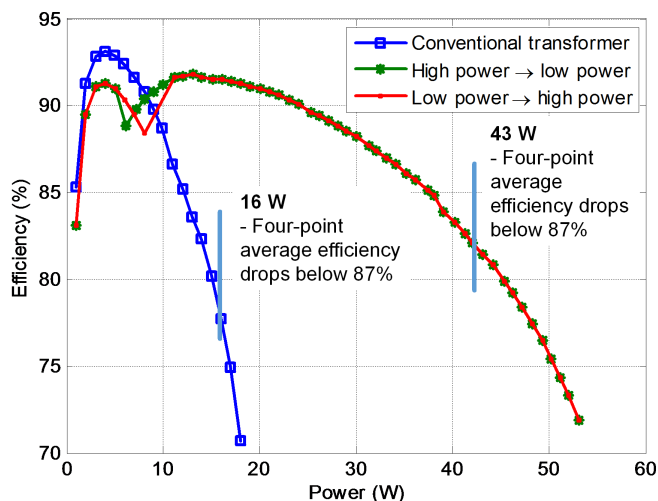


Fig. 7. Measured efficiency of the switched-winding transformer (red and green) and a conventional transformer (blue).

were measured with a resistive load. Table IV summarizes the performance of the switched-winding transformer and the comparison transformer with a single primary-secondary winding pair. Figure 7 illustrates the efficiency curve of the two transformers. The cycle in the curves of the switched-winding design (red and green) is due to the switching hysteresis required to prevent oscillation between states at power levels close to the transition point. The power ratings of both transformers are constrained by the Level VI efficiency standard. Figure 8 shows a thermal image of the prototype transformer under maximum load which illustrates that the system is not thermally constrained. The switched-winding transformer has an achievable power rating that is 227% of the power rating of the conventional design.

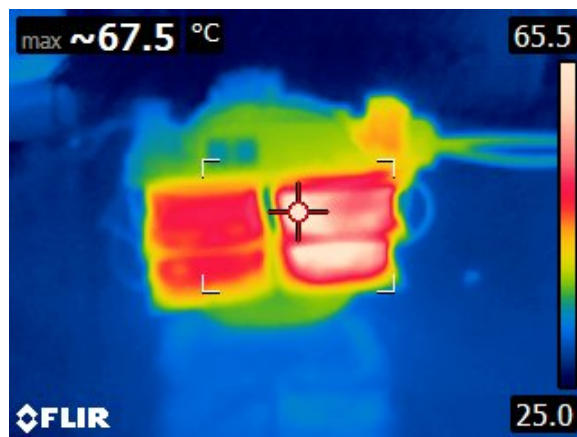


Fig. 8. Measured efficiency of the switched-winding transformer (red and green) and a conventional transformer (blue).

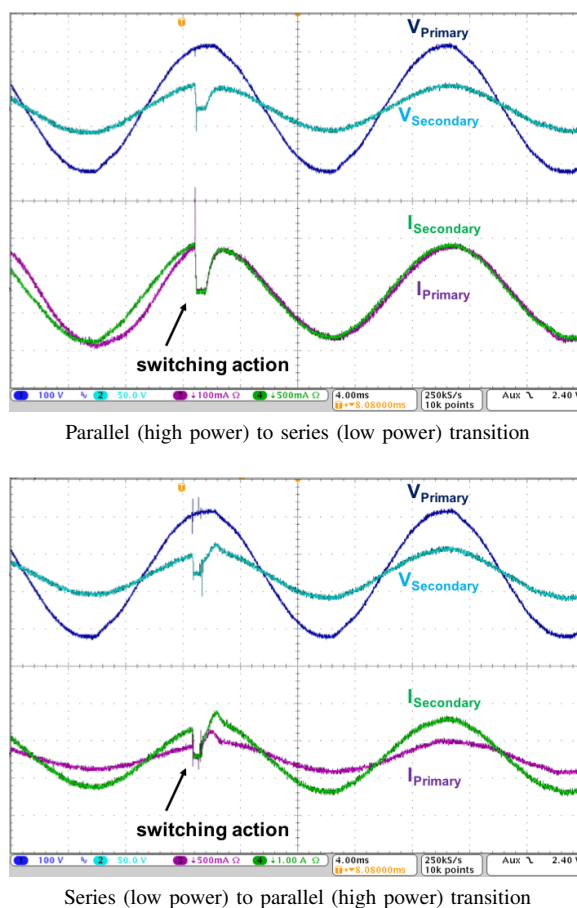


Fig. 9. Voltage and current waveforms during winding configuration transitions.

The reconfiguration process of the switched-winding transformer was evaluated to verify the timing of the switching at the peak of the line cycle and to monitor any voltage spikes or any inrush current associated with the reconfiguration. Figure 9 shows the high power to low power and low power to high power transitions with primary and secondary voltage and current.

As visible in the waveforms, there is an inductive voltage spike associated with each transition, primarily due to the

TABLE V
SWITCHED-WINDING TRANSFORMER COST ANALYSIS

Item	Cost
Relays	\$3.72
Microcontroller	\$1.14
Logic Power Supply	\$6.84
PCB	\$0.78
Other Passives	\$1.65
Core	\$3.70
Bobbin	\$0.89
Magnet Wire	\$7.44
Total	\$26.16

energy stored in the leakage inductance of the windings. This voltage spike is partially clamped by the bulk storage capacitor associated with the power supply for the control circuitry. There is a slight spike in current on the reconfiguration to the high power mode due to the temporary imbalance in flux density created by the transition. However, the amplitude of this spike is less than the peak current under heavy loading in normal operation.

The system was also tested under inductive and capacitive loads. Under these loads the system fails to correctly detect the point at which the transitions between high and low power modes should occur. This is because the phase shift in current with reactive loads disturbs the relationship between the ratio of primary and secondary voltage used for monitoring purposes and the true output power. A revised measuring method could utilize the ratio of the RMS primary and secondary voltages and work with a wide range of capacitive and inductive loading. However, it would also require additional calculations that would raise the power consumption of the microcontroller.

Additionally, due to the energy stored by inductive or capacitive loads, some of the switching transitions between the two modes generated transients large enough to reset the microcontroller. This could be mitigated with the addition of an output filtering network.

VI. COST ANALYSIS

Another metric that the system could be evaluated against would be a cost comparison with a traditional transformer. The reduction in size for a given power output that is achievable with the switched-winding method translates to a cost reduction for the 60Hz transformer, but also requires potentially costly control circuitry. Table V provides a cost breakdown of the switched-winding transformer using budgetary pricing in 1000 unit quantity.

Based on the previously derived scaling equation for copper loss, it can be estimated that the comparison transformer would need to be a least 360% larger to match the power output of the switched winding transformer. The closest available core set to this new scale costs \$7.41 in quantity while the magnet wire usage and cost can be assumed to scale roughly linearly, for a total transformer cost of \$34.19. Based on this

cost comparison, the switched-winding method would realize a cost savings with its total cost of \$26.16. However, this estimate is highly sensitive to the cost of magnet wire.

Cost savings for the switched winding transformer would focus on reducing the cost of the control circuitry. The greatest potential for cost savings is in the logic power supply which uses a low quiescent power DC/DC converter and large bulk storage ceramic capacitors, both of which significantly increase the bill-of-material (BOM) cost.

VII. CONCLUSION

This paper presents a switched-winding transformer system that allows for a significant reduction in size for transformers that are constrained by a limit on no-load power consumption. This approach is demonstrated with a prototype meeting the level VI efficiency standards with a nominal power output of 43 W at 24 V achieving 87.7% average efficiency. The switched-winding transformer has a power density 227% greater than a comparison transformer of similar weight and size. This significant increase in power density is achieved by splitting the transformer operation into a high-power state with optimized copper loss for loaded efficiency, and a low-power state with optimized core loss for low load or no-load operation. This implementation utilizes the transformer winding resistance to measure power output without the use of intrusive or expensive current sensors.

REFERENCES

- [1] Department of Energy, "Energy Conservation Program: Energy Conservation Standards for External Power Supplies", Available: https://www.energy.gov/sites/prod/files/2014/02/f7/eps_ecs_final_rule.pdf.
- [2] M. Zhu, K. Yu and F. L. Luo, "Switched Inductor Z-Source Inverter," *IEEE Transactions on Power Electronics*, vol. 25, no. 8, pp. 2150-2158, Aug. 2010.
- [3] B. Axelrod, Y. Berkovich and A. Ioinovici, "Switched-Capacitor/Switched-Inductor Structures for Getting Transformerless Hybrid DC-DC PWM Converters," *IEEE Transactions on Circuits and Systems I: Regular Papers*, vol. 55, no. 2, pp. 687-696, March 2008.
- [4] Y. Huo, T. Mattsson and P. Andreani, "A switched-transformer, 76% tuning-range VCO in 90nm CMOS," *2010 Asia-Pacific Microwave Conference*, Yokohama, 2010, pp. 1043-1046
- [5] S. P. Sah, D. Heo and S. Mirabbasi, "An inductively Gm enhanced 34-GHz VCO with gain linearization and switched transformer tuning," *2014 IEEE MTT-S International Microwave Symposium (IMS2014)*, Tampa, FL, 2014, pp. 1-4.
- [6] Jongwon Shin, Woosup Kim, Joung-Hu Park and Bo-Hyung Cho, "A new energy-recovery circuit for the plasma display panel using the switched transformer," *2008 IEEE Power Electronics Specialists Conference*, Rhodes, 2008, pp. 1857-1861.
- [7] K. Rustom, W. Qiu, C. Iannello and I. Batarseh, "Five-Terminal Switched Transformer Average Modeling and AC Analysis of PFC Converters," *IEEE Transactions on Power Electronics*, vol. 22, no. 6, pp. 2352-2362, Nov. 2007.
- [8] D. Nutt, "Reducing energy losses when transformers are lightly loaded," *IET Electric Power Applications*, vol. 1, no. 5, pp. 847-850, Sept. 2007.
- [9] A. Rand, "Inductor Size vs. Q: A Dimensional Analysis," *IEEE Transactions on Component Parts*, vol. 10, no. 1, pp. 31-35, Mar 1963.
- [10] C. R. Sullivan, B. A. Reese, A. L. F. Stein and P. A. Kyaw, "On size and magnetics: Why small efficient power inductors are rare," *International Symposium on 3D Power Electronics Integration and Manufacturing (3D-PEIM)*, Raleigh, NC, 2016, pp. 1-23.
- [11] R. W. Erickson and D. Maksimovic, "Basic Magnetics Theory," in *Fundamentals of Power Electronics*, Boston, MA, USA: Kluwer, 2001.